

Accepted and scheduled for publication in *the Astrophysical Journal*, for May 20, 2008, v 679 1 issue

## On the nature of the variability power decay towards soft spectral states in X-ray binaries. Case study in Cyg X-1

Lev Titarchuk<sup>1,2,3</sup> and Nikolai Shaposhnikov<sup>4</sup>

### ABSTRACT

A characteristic feature of the Fourier Power Density Spectrum (PDS) observed from black hole X-ray binaries in low/hard and intermediate spectral states is a broad band-limited noise, characterized by a constant below some frequency (a “break” frequency) and a power law above this frequency. It has been shown that the variability of this type can be produced by the inward diffusion of the local driving perturbations in a bounded configuration (accretion disk or corona). In the framework of this model, the perturbation diffusion time  $t_0$  is related to the phenomenological break frequency, while the PDS power-law slope above the “break” is determined by the viscosity distribution over the configuration. The perturbation diffusion scenario explains the decay of the power of X-ray variability observed in a number of compact sources (containing black hole and neutron star) during an evolution of these sources from low/hard to high/soft states. We compare the model predictions with the subset of data from Cyg X-1 collected by the Rossi X-ray Time Explorer (RXTE). Our extensive analysis of the Cyg X-1 PDSs demonstrates that the observed integrated power  $P_x$  decreases approximately as a square root of the characteristic frequency of the driving oscillations  $\nu_{dr}$ . The RXTE observations of Cyg X-1 allow us to infer  $P_{dr}$  and  $t_0$  as a function of  $\nu_{dr}$ . Using the inferred dependences of the integrated power of the driving oscillations  $P_{dr}$  and  $t_0$  on  $\nu_{dr}$  we demonstrate that the power predicted by the model also decays as  $P_{x,diff} \propto \nu_{dr}^{-0.5}$  that is similar to the observed  $P_x$ .

---

<sup>1</sup>George Mason University/Center for Earth Observing and Space Research, Fairfax, VA 22030; and US Naval Research Laboratory, Code 7655, Washington, DC 20375-5352; ltitarchuk@ssd5.nrl.navy.mil

<sup>2</sup>Dipartimento di Fisica, Università di Ferrara, via Saragat 1, I-44100, Ferrara, Italy; titarchuk@fe.infn.it

<sup>3</sup>Goddard Space Flight Center, NASA, code 661, Greenbelt MD 20771; lev@milkyway.gsfc.nasa.gov

<sup>4</sup>Goddard Space Flight Center, NASA/Universities Space Research Association, code 662, Greenbelt MD 20771; nikolai@milkyway.gsfc.nasa.gov

behavior. We also apply the basic parameters of observed PDSs, power-law index and low frequency quasiperiodic oscillations, to infer the Reynolds (Re) number from the observations using the method developed in our previous paper. Our analysis shows that Re–number increases from values about 10 in low/hard state to that about 70 during the high/soft state.

*Subject headings:* accretion, accretion disks—black hole physics—stars:individual (Cyg X-1) :radiation mechanisms: nonthermal—physical data and processes

## 1. Introduction

The main goal of the presented work is to explain a decay of the emergent time variability of X-ray emission in compact sources when these sources evolve from low/hard (LH) to high/soft (HS) states [see Remillard & McClintock (2006) and Titarchuk, Shaposhnikov & Arefiev (2007), hereafter TSA07, for details of observations]. In particular, power density spectrum (PDS) of black hole binaries in hard states is dominated by a component, which has a specific shape roughly described by a broken power-law. The low-frequency part is mostly flat, while the power-law index  $\alpha$  above the “break” frequency  $\nu_{br}$  is variable between 1 and 2. It is well established that the fractional root-mean-square (rms) variability in a source light curve decreases as a source evolves from LH state to HS state. Simultaneously, both  $\nu_{br}$  and  $\alpha$  increase. Although empirical shot-noise models were able to describe in general the observed PDS shape (Focke et al. 2005), the physical picture explaining the observed evolution during spectral transitions was missing. Moreover, shot-noise models were challenged by the linear absolute rms-flux relation (Uttley, McHardy & Vaughan 2005; Uttley 2004). This rms flux relation assumes that amplitudes and time-scales of shots are not independent, but are related in some way.

Lyubarskii (1997), hereafter L97, was the first to suggest a model for this time variability production in the accretion powered X-ray sources. He considered small amplitude local fluctuations in the accretion rate at each radius, caused by small amplitude variations in the viscosity, and then studied the effect of these fluctuations on the accretion rate at the inner disc edge. His linear calculations show that if the characteristic time-scale of the viscosity variations is everywhere comparable to the viscous (inflow) time-scale, and if the amplitude of the variations is independent of radius, then the power spectrum of luminosity fluctuations is a power-law  $1/\nu$ . If the amplitude of the variations increases with radius, the slope of the power spectrum of the luminosity variations is steeper than 1. Lyubarskii pointed out that he had no physical model for the cause of such fluctuations. Uttley, McHardy & Vaughan (2005) pointed out that rms-flux relation is naturally explained in the framework developed

by Lyubarskii.

TSA07 formulated and solved the problem of local driving perturbation diffusion in a “disk-like” configuration (which can be either a geometric thin Keplerian accretion disk or Compton cloud). The problem of the diffusive propagation of the space distributed high-frequency perturbations is formulated as a problem in terms of the diffusion equation for the surface density perturbations. This equation is combined with the appropriate boundary conditions. The formulation of this problem and its solution are general and classical. The parameters of the resulting PDS, diffusion time scale of the diffusion propagation of the local perturbations  $t_0$  and the power-law index of the viscosity distribution over radius, are essential parameters of diffusion in a given bounded configuration. In TSA07 we call our PDS model for the Green’s function of the bounded configuration as a white-red noise (WRN) and we adopt this name throughout this paper.

The problem formulation was similar to the Lyubarskii’s scheme. However, the method of solution is different. Lyubarskii treated the factorization of the driving term (i.e. separating it into two parts each depending on time and radius only) by linearizing the system. In TSA07 the analytical solution is obtained for the case of the factorized driving sources. Then, using the mean value theorem we showed that the general solution is simply a convolution of the configuration response signal (the Green’s function) and the mean driving signal in the configuration. Thus the resulting power spectrum of the X-ray signal, as a convolution, is a product of the power spectrum related to the configuration Green’s function and that related to the perturbation sources (sources of driving oscillations).

The PDS of the Green’s function is a white-red noise power spectrum (WRN). Specifically, the low frequency (LF) asymptotic form of the WRN PDS, when the frequency is less than the inverse of diffusion timescale in the “disk-like” configuration  $t_0^{-1}$ , is characterized by a flat shoulder (white noise). In other words, the LF white noise shoulder is insensitive to the source and viscosity distributions over radius. The high frequency (HF) asymptotic form of WRN is a power law  $\nu^{-\alpha}$  with index  $\alpha$ , which is determined by the viscosity and perturbation source distributions over the accretion configuration. The index  $\alpha = 3/2$  when the viscosity *linearly* increases with radius and the perturbation sources distribution is quasi-uniform. The basis of the presented power spectrum formation scenario is that the timing signal of the WRN PDS shape is a result of diffusive propagation of driving perturbations in the bounded configuration (disk or Compton cloud) in the same way as X-ray photon spectrum is a result of the photon diffusion (namely, upscattering of seed photons) in the same bounded configuration.

The driving oscillation amplitude is assumed to be a smooth function of the radius. TSA07 suggested that driving fluctuations in the configuration can be introduced by g-

mode driving oscillations at any given annulus. The local g-mode driving fluctuations, produced possibly by local Rayleigh-Taylor local instabilities, are high-frequency damped quasi-periodic oscillations (QPOs) which frequencies are related to the local Keplerian frequencies. As we mentioned above TSA07 formulated and solved a problem of the diffusive propagation of the space distributed high-frequency perturbations in the bounded configuration. Our diffusion model for PDS is a product of WRN PDS and the driving source PDS (Lorentzian).

The WRN PDS is a power spectrum of the solution of the initial value (Cauchy) problem which is a linear superposition of exponential shots [see Wood et al. (2001)]. For example, if the driving perturbations are distributed according to the first eigen-function of the diffusion operator then the bounded medium works as a filter producing just one exponential shot as a result of the diffusive propagation of eigen-function distribution of the seed perturbations. In the general case the resulting signal is a linear superposition of exponential shots which are *related* to the appropriate eigen-functions. Furthermore, TSA07 demonstrate that *the observed rms-flux relations* [e.g. Uttley, McHardy & Vaughan (2005)] is naturally explained by our diffusion model. In the framework of the linear diffusion theory the emergent perturbations are always linearly related to the driving source perturbations through a convolution of the configuration Green’s function and source distribution.

An important question is what our diffusion model predicts for relative contributions of the WRN PDS, the driving oscillation PDS in the resulting PDS and for a dependence of the integrated PDS power on the driving oscillation frequency. The next question is how this model dependence of the integrated power vs the driving oscillation frequency is related to the observed dependence of that. The answers to these questions are the points of the presented study.

In §2 we refer to details of Cyg X-1 observations with RXTE. In §3 we outline the main features of the diffusion model and related formulas. In §4 we show how the model integrated power vs the driving oscillation frequency fits X-ray data from Cyg X-1. In §5 we present the inferred correlation of the Reynolds number with the driving oscillation frequency and the spectral state (photon index). Application of the paper results to the observed index-QPO frequency correlations is considered in §6. Discussion and final conclusions follow in §7.

## 2. Observations

For our analysis we used Cyg X-1 data from the Proportional Counter Array (PCA) and All-Sky Monitor (ASM) onboard *RXTE* [Swank (1999)]. The data are available through the

GSFC public archive <sup>1</sup>. In this Paper we present the analysis of a representative subset of *RXTE* observations of Cyg X-1. A reader can find the details of data reduction and analysis in Shaposhnikov & Titarchuk (2006) and TSA07. We chose approximately 200 observations to cover the complete dynamical range of the source evolution from low/hard to high/soft state. For the presented analysis we refit PDSs with our new model and we used the results of our previous spectral analysis for photon index  $\Gamma$ .

To fit a PDS we used a sum of our perturbation diffusion model and one or two Lorentzians to account for the Low Frequency Quasi-Periodic Oscillations (LFQPOs). For higher photon indices, when the source is close to high/soft state, the contribution of the accretion disk variability component sometimes becomes significant. It is observed as an additional power law at the lower frequencies (see TSA07 for details). We fit this component with simple power law, when it is needed.

### 3. The main features of the model and underlying assumptions

We consider a scenario related to our model (see also TSA07) where the Compton Cloud ( “disk-like” configuration) is located in the innermost part of the source and the Keplerian disk is extended from the Compton Cloud (CC) to the optical companion [see Fig. 1 in Titarchuk, & Fiorito (2004), hereafter TF04, for the model geometry].

We remind the reader that the diffusion equation for the surface density perturbation is the same for any “disk-like” configuration for which the rotational frequency  $\Omega(R)$  as a function of radius  $R$  has a Keplerian-like profile namely  $\Omega \propto R^{-3/2}$  [see Wood et al. (2001) for details]. The standard Keplerian disk and ADAF kind of flow (Compton Corona) are particular examples of these accretion “disk-like” configurations.

The CC presumably contracts when the source goes to the softer state. TF04 infer that the CC cloud in low/hard state is about 40 Schwarzschild radii ( $R_S$ ) whereas that in high/soft state is about 4-5  $R_S$ . It is obvious that the variability of the mass accretion rate in the cloud leads to the variability of the gravitational energy release there.

The Earth observer sees this mass accretion rate ( $\dot{M}$ ) variation as a variability of X-ray flux coming from the source given that  $\dot{M}$  regulates the supply of the soft seed photons up-scattered off CC hot electrons. According to our scenario in the equatorial plane the plasma is more dense and consequently colder than that in the CC outer parts. The soft photons are produced in these relatively cold equatorial layers of CC and then they are Comptonized

---

<sup>1</sup><http://heasarc.gsfc.nasa.gov>

off hot electrons of the CC outer part forming the resulting X-ray spectrum.

Thus one can conclude that the variability of X-ray signal at energies higher than 3 keV (RXTE energy range) is mostly determined by the fluctuations of the luminosity  $\Delta L_x(t)$  originated in the CC. Here we study the luminosity fluctuations  $\Delta L_x(t)$  in the CC configuration.

We assume that the mass accretion rate variations  $\Delta \dot{M}(0, t)$  is converted with efficiency  $\varepsilon_{eff}$  into the variations of the X-ray luminosity, i.e.  $\Delta L_x(t) = \varepsilon_{eff} \Delta \dot{M}(0, t)$ . TSA07 show that the fluctuations of the resulting X-ray oscillation signal  $\Delta L_x(t)$  due to the diffusion of the driving perturbations is

$$\Delta L_x(t) = \int_0^t \varphi(t') Y(t - t') dt', \quad (1)$$

i.e. a convolution of the Green's function of the bounded configuration  $Y(t)$  (WRN) and the source variability function  $\varphi(t)$ . The resulting power spectrum is

$$\|F_x(\omega)\|^2 = \|F_\varphi(\omega)\|^2 \|F_Y(\omega)\|^2 \quad (2)$$

where  $F_x(\omega)$ ,  $F_\varphi(\omega)$ ,  $F_Y(\omega)$  are Fourier transforms of  $\Delta L_x(t)$ ,  $\varphi(t)$ ,  $Y(t)$  respectively. The WRN PDS  $\|F_Y(\omega)\|^2$  is described by Eq. (64) in TSA07 (also see the asymptotic forms of that in Eqs. 65-66 there).

Using the total power of the driving oscillations  $P_{dr}$  one can present the driving oscillation PDS as (see Eqs. 22 and B5 in TSA07)

$$\|F_\varphi(\nu)\|_\nu^2 = \frac{\hat{\Gamma}_{dr} P_{dr} / (a\pi)}{(\nu - \nu_{dr})^2 + (\hat{\Gamma}_{dr}/2)^2} \quad (3)$$

where  $\nu_{dr} = \omega_{dr}/(2\pi)$  is the driving oscillation frequency,  $\hat{\Gamma}_{dr}$  is a full width of half maximum (FWHM) of the Lorentzian and a constant  $a$  varies in the range between 1 and 2 depending on the ratio of  $2\nu_{dr}/\hat{\Gamma}_{dr}$ :

$$a = 1 + \frac{2 \arctan(2\nu_{dr}/\hat{\Gamma}_{dr})}{\pi}. \quad (4)$$

For example  $a = 1$  and  $a = 2$  when  $2\nu_{dr}/\hat{\Gamma}_{dr} \ll 1$  and  $2\nu_{dr}/\hat{\Gamma}_{dr} \gg 1$  respectively.

It is worth noting that Eqs (1-4) have been derived in TSA07 with an assumption that the local driving perturbations  $\Phi(t, \xi)$  are damped quasiperiodic oscillations, namely

$$\Phi(t, \xi) = A_\Phi f(\xi) \exp(-\frac{1}{2}\Gamma_{dr}t + i\omega_{dr}t) \quad (5)$$

where the amplitude of the driving oscillation is function of  $R$  only ( $\xi = R^{1/2}$ ). Note the damping coefficients  $\hat{\Gamma}$  in Eq. (3) and  $\Gamma$  in Eq. (5) are related as  $\Gamma = 2\pi\hat{\Gamma}$ .

Then TSA07 apply the mean-value theorem for the integral  $W(R, t)$  of Eq. B2 in TSA07. Namely the mean-value theorem in its general form for the product of two continuous functions  $g(t)$  and  $f(t)$  states that if a function  $g(t)$  is positive, i.e.  $g(t) > 0$  then

$$\int_a^b g(t)f(t)dt = f(x) \int_a^b g(t)dt$$

where  $a \leq x \leq b$ . Given that the product of the Green's function  $G(R, \xi, t)$  and the driving oscillation amplitude  $f(\xi)$  in Eq. B2 in TSA07 is positive we obtain that

$$W(R, t) = A_\Phi \int_0^t dt' \exp[-\Gamma_{dr}t'/2 + i\omega_{dr}(\xi_*)t'] \int_{R_{in}}^{R_0} G(R, \xi, t - t')f(\xi)d\xi$$

where  $R_{in} \leq \xi_* \leq R_0$ . Then TSA07 proceed with the Fourier transformation and PDS determination of  $W(R, t)$  and ultimately they derive equations (1-4).

In Fig. 1 we show a typical example of the model fit to the data using Eq. (2). The parameters of PDS continuum for white-red noise component (WRN)  $\|F_Y(\omega)\|^2$  (see for details TSA07) are the diffusion time scale  $t_0$ , index of the power-law viscosity distribution  $\psi$  and for the driving oscillation component  $\|F_\varphi(\omega)\|^2$  they are  $\nu_{dr}$  and  $\hat{\Gamma}_{dr}$  (see Eq. 3).

The power-law index of the viscosity distribution  $\psi$  is related to the power-law index of the red noise in the WRN PDS (see TSA07):

$$\alpha = \frac{3}{2} - \delta = \frac{16 - 5\psi}{2(4 - \psi)} \quad \text{for } \psi > 0$$

and

$$\alpha = 2 \quad \text{for } \psi < 0. \tag{6}$$

The model predicted integrated power is (see TSA07)

$$P_{x,diff} \sim \frac{P_{dr}}{2\pi\nu_{dr}t_0(\mathcal{Q} + 1/4\mathcal{Q})DC} \tag{7}$$

where  $\mathcal{Q} = \hat{\Gamma}_{dr}/\nu_{dr}$  is a quality factor for the driving signal and  $D$  is a factor of order of unity. Equation (7) was derived use the mean value theorem for the integral of the product of two functions. In TSA07 we assumed that a constant  $C$  related to the mean value of  $\|F_\varphi(\nu)\|_\nu^2$  over the frequency integration range is about a few (see Appendix B2 in TSA07 for details). Here we specify and obtain  $C$ -constant when we compare the model dependence  $P_{x,diff}$  on

$\nu_{dr}$  with the observable  $P_x$  on  $\nu_{dr}$ . In order to make this comparison one should determine the best-fit parameter  $t_0$  and  $P_{dr}$  as functions of  $\nu_{dr}$ . Note that to derive Eq. (7) we also use the fact that the WRN PDS  $\|F_Y(\omega)\|^2$  is normalized to  $1/(Dt_0)$  where  $D \gtrsim 1$ . (see Eq. B16 in TSA07).

Now we follow the method suggested in TSA07 to infer  $P_{dr}$  vs  $\nu_{dr}$  from the observations. Namely, given the fact that the driving PDS is a constant at frequencies  $\nu \ll \nu_{dr}$  we have

$$\|F_\varphi(\nu)\|_\nu^2 = \|F_\varphi(0)\|_\nu^2 = \frac{\hat{\Gamma}_{dr} P_{dr} / (a\pi)}{\nu_{dr}^2 + (\hat{\Gamma}_{dr}/2)^2}. \quad (8)$$

Because for any power spectrum  $\|F(\omega)\|^2$

$$\|F(\omega)\|^2 d\omega = \|F(2\pi\nu)\|^2 2\pi d\nu = \|F(\nu)\|_\nu^2 d\nu$$

we obtain that (compare with Eq. 2)

$$\|F_x(\nu)\|_\nu^2 = (2\pi)^{-1} \|F_\varphi(\nu)\|_\nu^2 \|F_Y(\nu)\|_\nu^2. \quad (9)$$

Thus a combination of Eqs. (8) and (9) leads us to determination of the integrated power of the driving oscillations

$$P_{dr} = \frac{a\pi(\nu_{dr}^2 + (\hat{\Gamma}_{dr}/2)^2)}{\hat{\Gamma}_{dr}} \|F_\varphi(0)\|_\nu^2 = 2\pi^2 a \frac{\nu_{dr}^2 + (\hat{\Gamma}_{dr}/2)^2}{\hat{\Gamma}_{dr}} \frac{\|F_x(0)\|_\nu^2}{\|F_Y(0)\|_\nu^2}. \quad (10)$$

We remind a reader that the values of  $\nu_{dr}$  and  $\hat{\Gamma}_{dr}$  are the best-fit PDS parameters,  $\|F_x(0)\|_\nu^2$  is the observed PDS value at  $\nu = 0$  and  $\|F_Y(0)\|_\nu^2$  is a value of the normalized WRN PDS at  $\nu = 0$ . As we mention above the integral of the normalized WRN PDS  $\|F_Y(\nu)\|_\nu^2$  over  $\nu$  is  $1/(Dt_0)$ .

#### 4. The integrated power vs driving oscillation frequency and photon index

In Figure 2 we present the observed correlation of low frequency QPO centroid  $\nu_L$  with the driving QPO frequency  $\nu_{dr}$  (upper panel) and photon index  $\Gamma$  with  $\nu_{dr}$  (lower panel). These correlations imply that  $\nu_L$  along with  $\nu_{dr}$  increase when the source becomes softer. In other words, the emission area [Compton cloud (CC)] contracts when the source evolves to the soft states.

In Figure 3 we also see this effect of CC contraction as anticorrelation of the CC diffusion time scale  $t_0$  with  $\nu_{dr}$ . The inferred dependence of  $t_0$  vs  $\nu_{dr}$  can be fitted by the power law  $t_0 \propto \nu_{dr}^{-2.13 \pm 0.14}$ .



We infer the integrated power of the driving oscillations  $P_{dr}$  vs  $\nu_{dr}$  (see Eq. 10) and then we obtain the model integrated power  $P_{x,diff}$  vs  $\nu_{dr}$  (see Eq. 7). In Figure 4 we show that the dependence of  $P_{dr}$  vs  $\nu_{dr}$  can be fitted by power law  $P_{dr} \propto \nu_{dr}^{-1.8 \pm 0.16}$ . Namely the driving oscillation power  $P_{dr}$  decreases when the source (Cyg X-1) goes to softer states. Presumably the decay of  $P_{dr}$  with  $\nu_{dr}$  is also related to the contraction of Compton cloud. The driving oscillations can result from the Rayleigh-Taylor (RT) local instability [see e.g. Chandrasekhar (1961) and Titarchuk (2003)]. The decay of  $P_{dr}$  can be considered as a cumulative effect of the local Rayleigh-Taylor (RT) instability when the effective area of a given configuration (CC) undergoing RT oscillations contracts.

In Figure 5 we present a comparison of the observable PDS integrated power  $P_x$  (black filled circle) with the model predicted  $P_{x,diff}$  (crosses) (see Eq. 7). One can see that the dependence  $P_{x,diff}$  on  $\nu_{dr}$  is similar to the observable correlation  $P_x$  vs  $\nu_{dr}$ .

Note that we obtain the factor  $C \sim 4$  (see Eq. 7) by shifting a set of the values of  $P_{x,diff}$  along Y-axis to fall on top of  $P_x$  values. The power-law  $P_x \propto \nu_{dr}^{-0.48 \pm 0.03}$  fits the dependence of the theoretical and observable integrated powers vs the driving oscillation frequency.

## 5. The Reynolds number of the accretion flow in Compton cloud configuration

Titarchuk, Lapidus & Muslimov (1998), hereafter TLM98 introduced the Reynolds number  $Re = V_R R / \hat{\nu}$  ( $\gamma$  in their notation) where  $V_R$ ,  $\hat{\nu}$  are an average radial velocity, an average viscosity over a given configuration respectively and  $R$  is a configuration scale. They demonstrate that the size of the transition layer (CC) between the fast rotating accretion disk and the relatively slow rotating central object (either BH or NS) strongly depends on the Reynolds number  $Re$ . It is worth noting that  $\alpha$ -viscosity parameter introduced by Shakura & Sunyaev (1973) is related to the TL (CC) parameter  $Re$ . Given that  $\alpha \sim \hat{\nu} / (V_s H)$ , where  $V_s$  is the sound velocity in the “disk-like” configuration and  $H$  is a half of the configuration vertical size, we obtain that

$$Re \sim \lambda / \alpha. \quad (11)$$

To infer this formula one should assume that  $\lambda = H/R$  and  $V_s \sim V_R$ .

TSA07 has already shown that there is a possibility to infer  $Re$ , and consequently  $\alpha$ -parameter (see Eq. 11), using the RXTE observations of BHs and NSs. This determination can be done if a particular RXTE power spectrum (PDS) has the white-red noise (WRN) component and also if the QPO low frequency  $\nu_L$  is present there. TSA07 argue that the relation between observed frequencies  $\nu_L$  and  $1/t_0$  seen in Cyg X-1 PDSs is similar to the theoretical relation between the diffusion frequency  $\nu_{diff}$  and the frequency of CC volume

(magneto-acoustic) oscillations  $\nu_{MA}$  [see e.g. Titarchuk, & Osherovich (1999)]. This fact leads them to conclude that  $\nu_L$  can be considered as the frequency of the magneto-acoustic oscillations which theory was developed by Titarchuk et al. (2001), hereafter TBW01.

Using the best-fit parameters of the PDSs we can even infer the evolution of the Reynolds number of the accretion flow in the Compton cloud (CC), with the change of photon index  $\Gamma$ . In fact, TSA07 relate diffusion time  $t_0$  with Re and a magneto-acoustic QPO frequency  $\nu_{MA}$  as

$$t_0 = \frac{4}{3} \frac{4}{(4-\psi)^2} \left[ \frac{V_R R_0}{\hat{v}(R_0)} \right] \left( \frac{R_0}{V_R} \right) = \frac{4}{3} \frac{4}{(4-\psi)^2} \frac{\text{Re}}{a_{MA} \nu_{MA}}, \quad (12)$$

where  $V_R \sim V_s$  and  $a_{MA}$  is a numerical coefficient. Formula (12) leads to the equation

$$\text{Re} = 2\pi \left( \frac{a_{MA}}{2\pi} \right) \frac{3(4-\psi)^2}{4} (\nu_L t_0) \quad (13)$$

that allows us to infer a value of Re using the best-fit model parameters  $t_0$  and the QPO low frequency  $\nu_L$  which is presumably close to  $\nu_{MA}$ . Ultimately we can find the evolution of Re with the photon index  $\Gamma$  given that  $\nu_L$ ,  $t_0$  and the viscosity index  $\psi$  evolve with  $\Gamma$  (see Figs. 2-3 and 6).

In Figure 7 we present the inferred Reynolds number as a function of the photon index  $\Gamma$ . We use Eq. (13) where we set  $a_{MA} = 2\pi$  (see details of this determination of  $a_{AM}$  in TBW01 and TSA07) and the observable correlations of  $\nu_L$  and  $t_0$  with  $\Gamma$  (see Figs. 2 and 3). One can see that Re-number steadily increases from 10 to 70 when the source evolves from low/hard state to high/soft state. In contrast, TSA07 found that  $\text{Re} \sim 8 \pm 2.5$ . We note, however, that in TSA07 only WRN model was used without accounting for driving oscillation distribution, which significantly affects the resulting value for  $\psi$ . They also used a limited set of data.

Note the observed behavior of the Re-number vs  $\Gamma$  and mass accretion rate was predicted by TLM98, where they formulated a transition layer model (TLM) and studied its consequences for observations. It is important to emphasize that the Re-number along with the photon index  $\Gamma$ , the low frequency QPO  $\nu_L$  and the driving frequency  $\nu_{dr}$  can be considered as characteristics of the spectral state. All of them correlate with each other.

## 6. Photon index-QPO frequency correlation

TLM98 showed that the outer (adjustment) radius of the transition layer (CC)  $R_{out}$  measured in the dimensionless units with respect to Schwarzschild radius  $R_S = 2GM/c^2$ ,  $r_{out} = R_{out}/R_S$ , anticorrelates with Re-number or photon index  $\Gamma$  (spectral state) only. Thus

$\nu_L$  (or  $\nu_{MA}$ ) as a ratio  $\sim V_{MA}/R_{out}$  should correlate with  $\Gamma$  (or Re–number) where values  $\nu_L$  related to the same  $\Gamma$  for different sources should be inversely proportional to a mass of the central object (black hole or neutron star). Note that a plasma velocity  $V_{MA}$  is also a function of  $\Gamma$  only. The comparison of the observed index–QPO frequency correlations for two different sources (with two different masses) should lead to determination of their relative masses with respect each other. This is the main idea behind the method of weighing black holes (TLM98) recently applied for BH mass determination in a number of Galactic and extragalactic sources [see TF04; Fiorito & Titarchuk (2004); Dewangan, Titarchuk & Griffiths (2006); Strohmayer et al. (2007) and Shaposhnikov & Titarchuk (2007)].

## 7. Discussion and Conclusions

Chakrabarti & Titarchuk (1995) proposed a model of the truncated Keplerian disk and hot corona located in the innermost part of the source using arguments in terms of radiation hydrodynamics. Churazov et al. (1999), hereafter CGR99, were the first who supported this model using the specific form of the power spectra of X-ray radiation. Particularly they noted that two-component X-ray spectra (soft multicolour black-body and harder power law) are frequently observed from accreting black holes. These components are presumably associated with the different parts of the accretion flow (optically thick and optically thin respectively) in the vicinity of the compact source. They also emphasized that for Cygnus X-1, the overall shape of the power density spectra in the soft and hard spectral states can be *qualitatively* explained if the geometrically thin disc is sandwiched by the geometrically thick corona extending in a radial direction up to a large distance from the compact object. In the hard state the thin disc is truncated at some distance from the black hole followed by the geometrically thick flow. The break in the PDS is then associated with the characteristic frequencies in the accretion flow at the thin disc truncation radius.

However there is a difference between CGR99’s suggestions and the results of our paper. We come to the model of the truncated disk plus corona using the fit of the theoretical model of the power spectrum (see TSA07) to the data. Whereas CGR99 proposed a *qualitative* explanation of the data using Lyubarskii’s idea on the formation of the power spectrum in X-ray binaries [see L97].

Our results confirm the CGR99 conclusion that a stable optically thick (but geometrically thin) disk extends down to small radii (as indicated by the strong and stable soft component) and whereas prominent variations of the harder component (presumably related to Compton cloud) are present in the broad range of time-scales (up to at least  $10^2$  s; see Figs. 2-3 in TSA07). We also confirm the observed emergent spectrum consisting of two compo-

nents (soft stable component due to the disc emission and harder highly variable component due to Comptonization in the corona). The relative contribution of these two components to the luminosity of an averaged spectrum would then reflect the ratio of the energy releases in the disc and corona (or mass accretion rates). It is also worth noting that our presented analysis indicates that the high-frequency part of the PDS (QPO and turnover) at about 10 Hz and higher is possibly related to the local instabilities operating in the Comptonization region of the energy release (see CGR99). Note that Gierlinski & Zdziarski (2005) also pointed out the evolution of PDSs in XTE J15550-564 and XTE J1650-500. In particular they showed a variable power in the Comptonized component (the PDS high-frequency component) when a given source evolves from hard to soft states.

However there is a difference in details between the CGR99 and results of our papers (see also TSA07). For example the break in the PDS frequency range between 0.01 and 1 Hz is associated with the characteristic diffusion frequencies of the Compton cloud but not as that in CGR99 “with the characteristic frequencies in the accretion flow at the thin disc truncation radius.”

Axelsson et al. (2005), hereafter ABL05, suggested a model of the PDS of Cyg X-1 which successfully presented a natural transition from hard state through intermediate state to soft state and back, and also allowed them to study the behavior of the Lorentzian components in detail. Using this model consisting of a power-law and two Lorentzian profiles, ABL05 were able to fit the Cyg X-1 PDSs, and to follow the components from hard state through the transitions and back. By choosing this simple empirical approach for the PDS data analysis ABS05 could model the major features in all states with only three components. The parameters used in ABL05 were the width and peak frequency of the Lorentzians, along with the power at the peak frequency, The parameter evolution and its correlation between each other can all be described by continuous functions.

However ABL05 did not address to the nature of the components and continuum of the power spectrum. Their PDS description was pure phenomenological (compare with that in TSA07 and this paper).

ABL05 also showed that the PDS of Cyg X-1 is dominated by the same two Lorentzian components at all times. They came to this conclusion based on the fact that the relation of the peak frequencies of these Lorentzian components follows the pattern seen in both other BH and NS systems, and therefore they proposed that the physical processes responsible for them cannot be explained by invoking magnetic fields, a solid surface, or an event horizon.

It is worth noting that we also find that the diffusion (break) and QPO frequency follows the BH-NS pattern (see details in ST06 and TSA07). In addition to this we demonstrate that

there is a certain correlation between QPO low frequency and driving (high) frequency and photon index (see Fig. 2) and show a correlation between the diffusion time scale (an inverse of the diffusion frequency) and the driving frequency (see Fig. 3). Furthermore we explain the nature of the observational appearances of the power and photon spectra evolution by the evolution of the truncated disk and corona configurations when a X-ray source evolves from hard state to soft states. We come to the conclusion that the truncated disk and corona scenario should be a common model in BH and NS systems.

In fact, TLM98 showed that the bounded configuration (Compton cloud) surrounding compact objects is the transition layer (TL) that is formed as a result of dynamical adjustments of a Keplerian disk to the innermost sub-Keplerian boundary conditions. They argued that this type of adjustment is a generic feature of the Keplerian flow in the presence of the sub-Keplerian boundary conditions near the central object and that it does not necessarily require the presence or absence of a hard surface. TLM98 concluded that an isothermal sub-Keplerian TL between the NS surface and its last Keplerian orbit forms as a result of this adjustment. The TL model is general and is applicable to both NS and BH systems.

As the conclusions we want to single out

1. That we explain the decay of the emergent time variability of X-ray emission in compact sources when these sources evolve from low/hard to high/soft states. We find that the resulting power  $P_x$  from Cyg X-1 decays with the driving oscillation frequency  $\nu_{dr}$  as  $P_x \propto \nu_{dr}^{-0.5}$ .

2. We show that the reciprocal of the diffusion time scale of the perturbation  $t_0^{-1}$ , the low frequency QPO  $\nu_L$ , the driving oscillation frequency  $\nu_{dr}$ , inferred by fitting the Cyg X-1 PDSs with our diffusion model, increase when the source evolves from low/hard state to high/soft state. This behavior of the PDS characteristics implies that the Compton cloud contracts towards softer spectral states. The driving oscillations are probably caused by the local Rayleigh-Taylor instability which cumulative  $P_{dr}$  decreases when the effective area of the configuration producing the RT oscillations contracts. The decay in driving power leads to the decay in the total observed variability power from the source. Using the fact that  $t_0^{-1}$ ,  $\nu_L$ ,  $\nu_{dr}$  increase with  $\Gamma$  and  $P_{dr}$ ,  $P_x$  decrease with  $\Gamma$  we conclude, as a result of our analysis, that the Compton Corona shrinks when Cyg X-1 goes from low/hard state to high/soft state.

3. Our extensive data analysis of the power spectra from Cyg X-1 with an application of the method of Re–number determination developed in TSA07 indicates that Re related to Compton cloud configuration increases from values about 10 in low/hard state to that about 70 in high/soft state. We confirm the predictions by TLM98 that Re–number should increase with index and QPO frequencies. Thus one can conclude that the observable index-

QPO correlation is probably driven by the increase of Re–number when the source evolves from low/hard state to high/soft state. It is worth noting that inverse proportionality of the low-frequency QPO with respect BH mass in the index-QPO correlation leads to the method weighing BHs employing this index-QPO correlation.

We acknowledge very useful comments and suggestions by the referee.

## REFERENCES

- Axelsson, M., Borgonovo, L. & Larsson, S. 2005, *A&A*, 438, 999 (ABL05)
- Chandrasekhar, S. 1961, *Hydrodynamics and Hydromagnetic Stability*, Oxford: Oxford at the Caredon Press
- Chakrabarti, S.K. & Titarchuk, L. 1995, *ApJ*, 455, 623
- Churazov, E., Gilfanov, M. & Revnivtsev, 1999, *MNRAS*, 321, 759 (CGR99)
- Dewangan, G., Titarchuk, L. & Griffiths, R. 2006, *ApJ*, 637, L21
- Fiorito, R., Titarchuk, L. 2004, *ApJ*, 614, 2, L113
- Focke, W. B., Wai, L. L., & Swank, J. H. 2005, *ApJ*, 633, 1085
- Gierlinski, M. & Zdziarski, A. 2005, *MNRAS*, 370, 837
- Lyubarskii, Yu., E. 1997, *MNRAS*, 292, 679 (L97)
- Remillard, R. A. & McClintock, J. E. 2006, *ARA&A*, vol. 44, 49
- Shakura, N. I. & Sunyaev, R. A. 1973, *A&A*, 24, 337 (SS73)
- Shaposhnikov, N. & Titarchuk, L. 2007, *ApJ*, 663, 445
- Shaposhnikov, N. & Titarchuk, L. 2006, *ApJ*, 643, 1098
- Strohmayer, T. E., Mushotzky, R. F., Winter, L., Soria, R., Uttley, P., & Cropper, M. 2007, *ApJ*, 660, 580
- Swank, J. H. 1999, *Nucl. Phys. B - Proc. Suppl.*, 69, 12, 569, 362
- Titarchuk, L., Shaposhnikov, N. & Arefiev, V. 2007, *ApJ*, 660, 556 (TSA07)
- Titarchuk, L. 2003, *ApJ*, 591, 354

- Titarchuk, L.G., Bradshaw, C.F., & Wood, K.S. 2001,  
Titarchuk, L.G. & Fiorito, R. 2004, ApJ, 612, 988 (TF04)  
Titarchuk, L., Lapidus, I.I., & Muslimov, A. 1998, ApJ, 499, 315 (TLM98)  
Titarchuk, L.G. & Osherovich, V.A. 1999, ApJ, 518, L95  
Uttley, P., McHardy, I.M., & Vaughan, S. 2005, MNRAS, 359, 345  
Uttley, P. 2004, MNRAS, 347, L61  
Wood, K. S., Titarchuk, L., Ray, P.S., et al. 2001, ApJ, 563, 246 (W01)

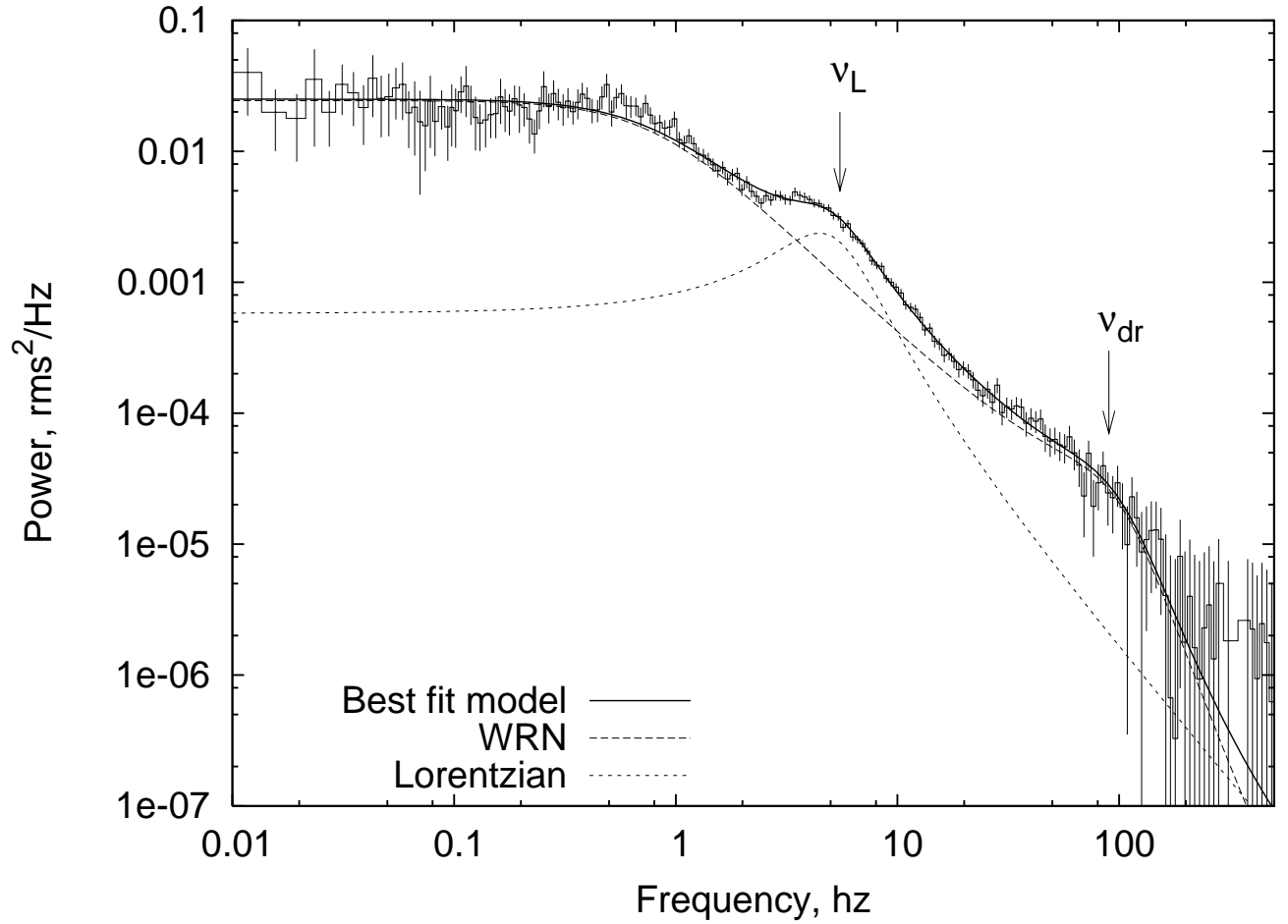


Fig. 1.— A particular example of observable PDS. The PDS continuum is fitted by our diffusion PDS model which is a product of WRN PDS and the driving oscillation Lorentzian. We also use a simple Lorentzian to fit QPO features.



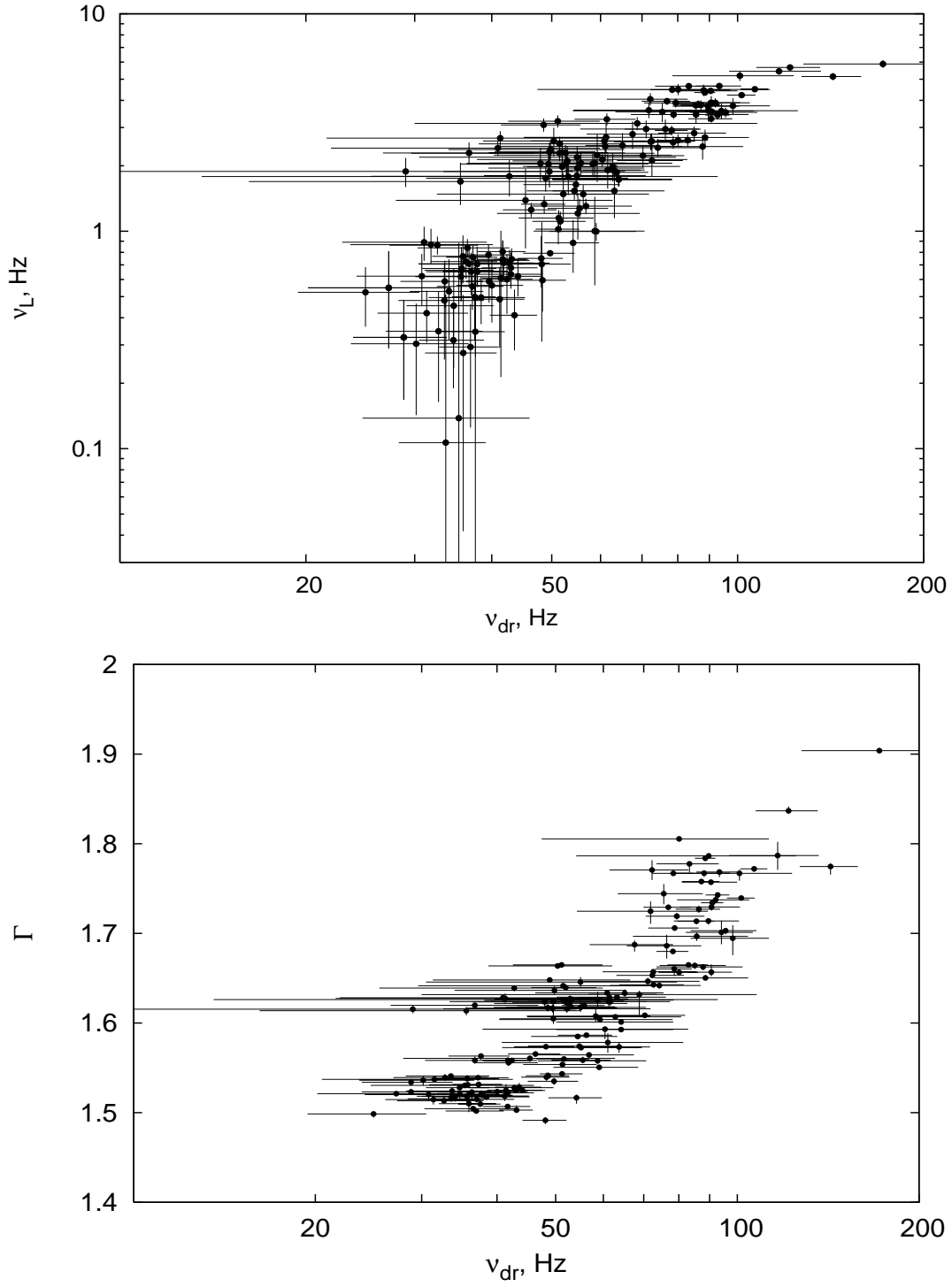


Fig. 2.— Upper panel: low QPO frequency  $\nu_L$  vs driving QPO frequency  $\nu_{dr}$  lower panel: photon index  $\Gamma$  vs  $\nu_{dr}$  .

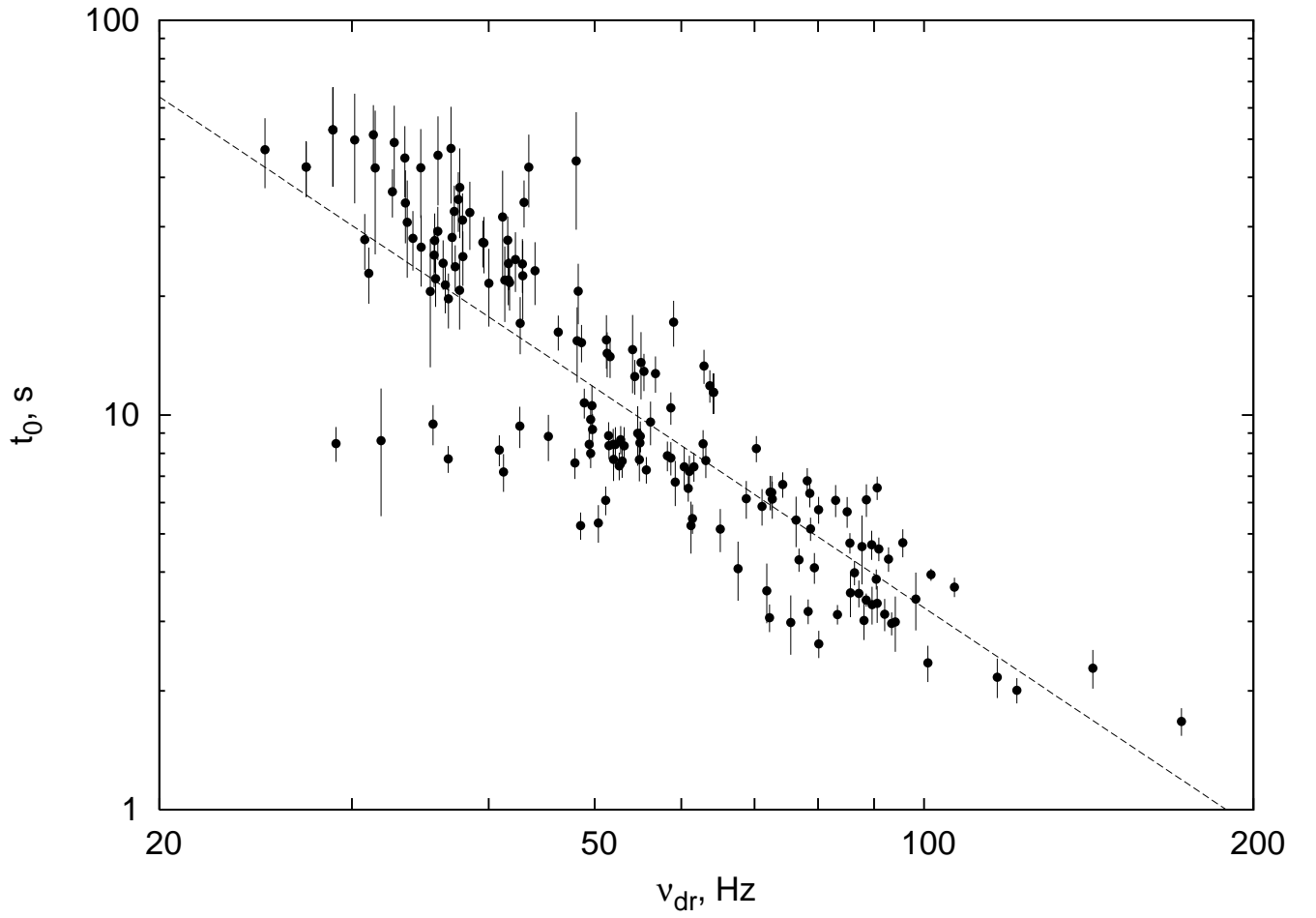


Fig. 3.— The best-fit model parameter, diffusion time scale  $t_0$  vs  $\nu_{dr}$ . The dashed line is the best fit power law  $t_0 \propto \nu_{dr}^{-2.13 \pm 0.14}$ .

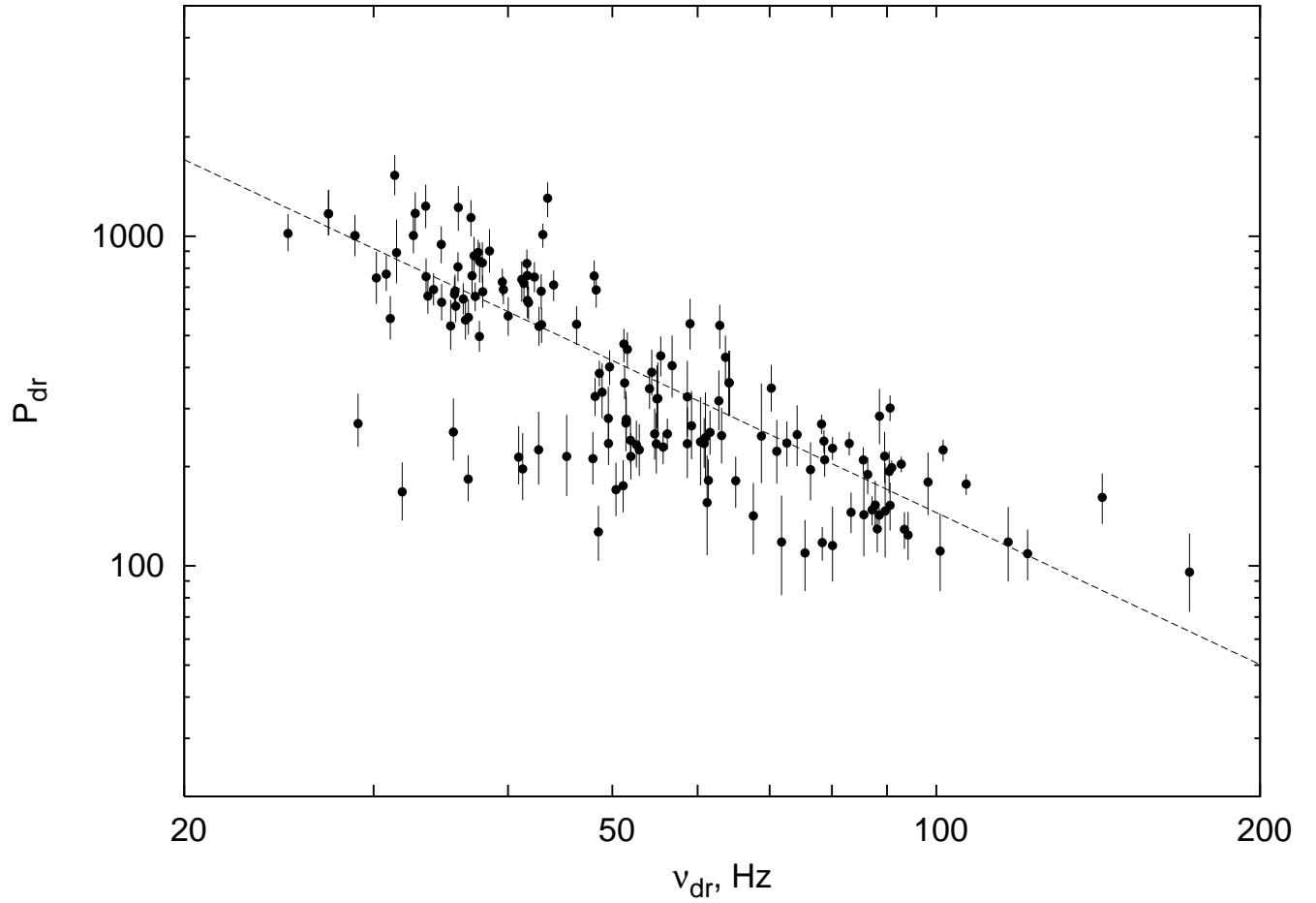


Fig. 4.— Inferred  $P_{dr}$  vs  $\nu_{dr}$ . The dashed line is the best fit power law  $P_{dr} \propto \nu_{dr}^{-1.8 \pm 0.16}$ .

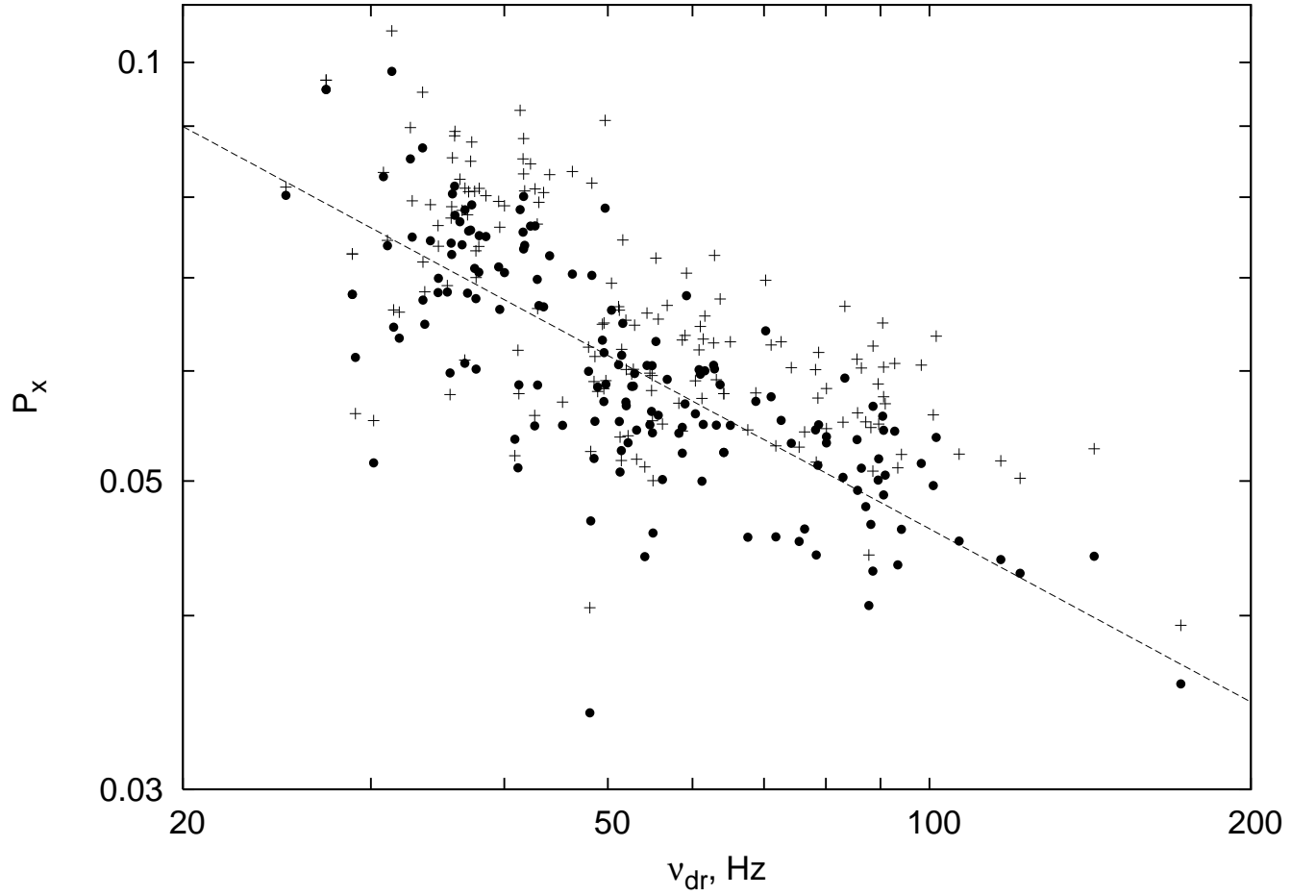


Fig. 5.— Comparison of the model  $P_{x,diff}$  vs  $\nu_{dr}$  (crosses) (using Eq. 7) with the observable  $P_x$  vs  $\nu_{dr}$  (black filled circle) The dashed line is the best-fit power law  $P_x \propto \nu_{dr}^{-0.48 \pm 0.03}$ .

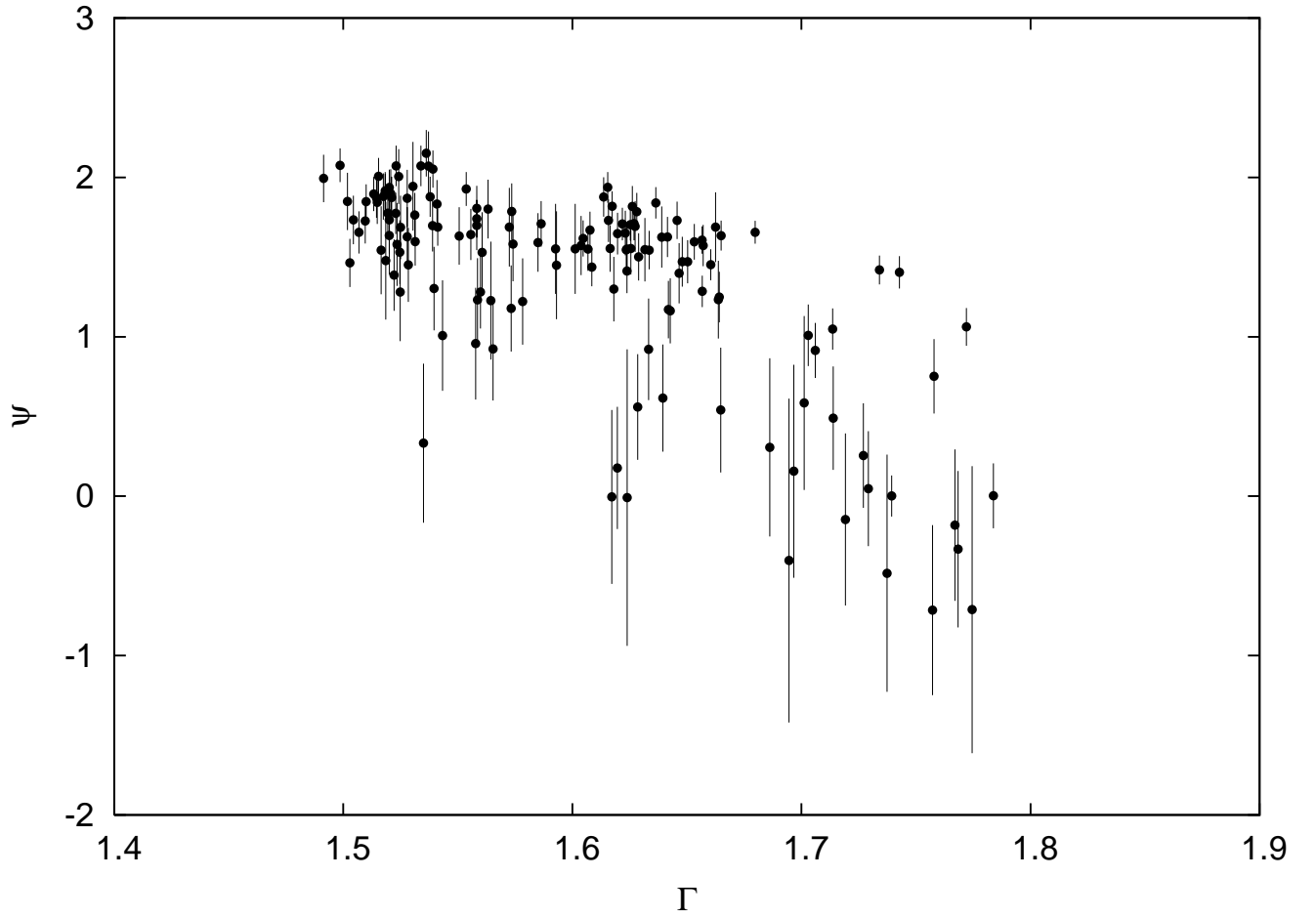


Fig. 6.— The best-fit index of the viscosity distribution  $\psi$  vs  $\Gamma$ .

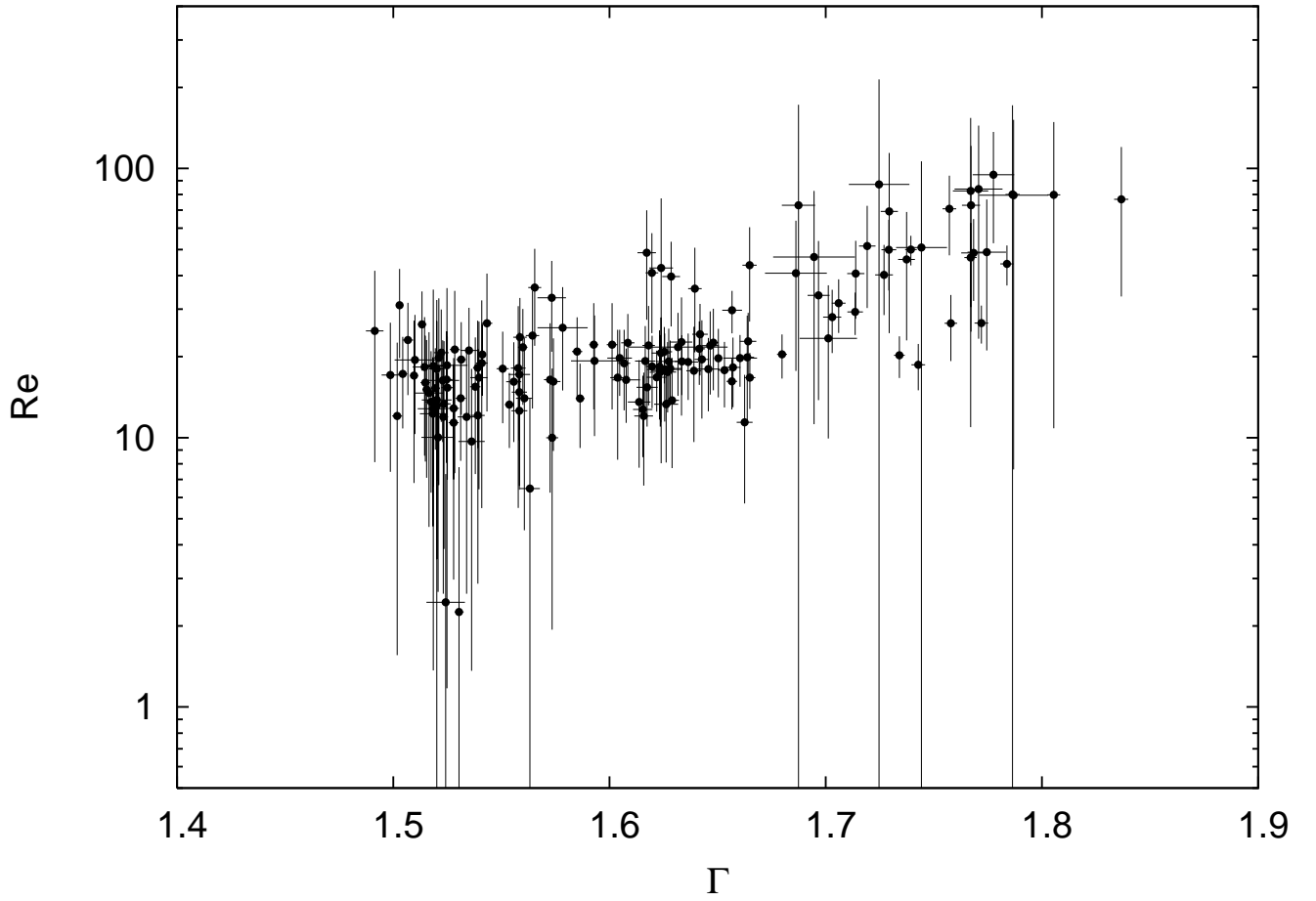


Fig. 7.— Inferred Reynolds number  $Re$  (using  $t_0$ ,  $\nu_L$ ,  $\psi$ , and Eq. 13) vs  $\Gamma$ .